

# A fast noise filtering algorithm for time series prediction using recurrent neural networks

Boris Rubinstein,  
Stowers Institute for Medical Research  
1000 50th St., Kansas City, MO 64110, U.S.A.

March 24, 2022

## Abstract

Recent research demonstrate that prediction of time series by recurrent neural networks (RNNs) based on the noisy input generates a *smooth* anticipated trajectory. We examine the internal dynamics of RNNs and establish a set of conditions required for such behavior. Based on this analysis we propose a new approximate algorithm and show that it significantly speeds up the predictive process without loss of accuracy.

## 1 Introduction

Recurrent neural networks (RNNs) due to their ability to process sequences of data have found applications in many fields of science, engineering and humanities, including speech, handwriting and human action recognition, automatic translation, robot control etc. One of the RNN application is time series prediction used in analysis of business and financial data, anomaly detection, weather forecast. A large number of different architectures were discussed recently and the flow of new modifications of standard RNN continues to increase and all these architectures share some common features inherited from the basic systems.

Trajectory prediction based on incomplete or noisy data is one of the most amazing features of organism brains that allows living creatures to survive in complex and mostly unfriendly environment. A large number of mathematical algorithms developed for this purpose have many applications in multiple engineering field, e.g., development of guidance systems, self-driving vehicles, motor control etc. [1].

It was shown that when the input signal represents a chaotic dynamics (in discrete or discretized continuous setting) RNNs indeed predict chaotic attractor for some number of steps and then the predicted trajectories diverge from the actual ones [2–4]. This result seems natural as it reflects an important property of chaotic dynamics – extremely high sensitivity of chaotic systems to small perturbations in initial conditions.

What does happen when a trajectory is perturbed by external noise of specific statistics, e.g., white noise? How would RNN extrapolate the input of such noisy time series? Generally speaking, when a noisy signal is used as an input to a *predictive* RNN it is expected that a trained network would be able to extrapolate the *noisy* time series. It appeared that the extrapolated trajectory is not noisy – filtering of the noisy perturbation of the Lorenz attractor dynamics was reported in [5] where the authors used recurrent multi-layer perception network and noted that the reconstructed signals were “reasonably close to the noise-free signal and the iterated predictions are smoother in comparison to the noisy signals” [5]. This observation leads to the following question - given a smooth deterministic function with added noise component as a RNN input will the trajectory anticipated by RNN be noisy or smooth? A short note [6] considered LSTM network with 128 neurons trained on the Mackey-Glass time series with added noise and demonstrated that with the increase of the noise level LSTM behaviour depends more on its own dynamics than on the input data. On the contrary, the training using the noiseless input produces RNN with very high sensitivity to small perturbations.

In this manuscript we attempt to explain the fact that RNN trained on segments of *noisy* trajectory and being fed a segment of such trajectory generates a *smooth* extrapolating curve. Our analysis shows that smooth predictions are commonplace and independent of the RNN type or extrapolation quality. We establish conditions for such RNN behavior and find that when these conditions are met a new very fast

predictive algorithm can be implemented. We demonstrate that this algorithm for relatively long input sequences (around 100 time points) works as good as the original one and gives the speed up to two orders of magnitude.

The manuscript is organized as follows. Section 2 describes the architecture of a very simple network made of a single recurrent network with small number of neurons followed by a linear layer. Section 3 describes RNN governing transformations and presents a standard algorithm used for time series prediction. Next Section 4 deals with the network training and discusses the dependence of the prediction quality on the number of neurons in RNN. Section 5 considers the input noise influence onto RNN state dynamics and demonstrates that it cannot be neglected. Then in Section 6 the focus shifts to the RNN dynamics during a recursive prediction procedure and conditions when this procedure results in smooth output are established. We show that satisfaction of these conditions allows to design a new much faster predictive algorithm described in details in Section 7 and demonstrate its high quality of extrapolation. Section 8 is devoted to discussion of possible applications and generalizations of our findings.

## 2 Network architecture and predictive algorithm

Consider a simple two layer network designed to predict multidimensional time series  $\mathbf{X} = \{\mathbf{x}_i\}$ ,  $1 \leq i \leq N$ . The first layer is a recursive network with  $n$  neurons – it takes a subsequence  $\mathbf{X}_{k,m} = \{\mathbf{x}_i\} = \{\mathbf{x}_{k+1}, \mathbf{x}_{k+2}, \dots, \mathbf{x}_{k+m}\}$ ,  $0 \leq k \leq N - m$ , of  $m$  vectors  $\mathbf{x}_i$  having dimension  $d$  each and returns a sequence  $\mathbf{S}$  of  $n$ -dimensional state vectors  $\mathbf{s}_i$ , ( $1 \leq i \leq m$ ). The last element  $\mathbf{s}_m$  is transferred into the second linear layer that generates an output vector  $\bar{\mathbf{x}}$  of dimension  $d$  by linear transformation  $\bar{\mathbf{x}} = \mathbf{W} \cdot \mathbf{s}_m + \mathbf{b}$ , with matrix  $\mathbf{W}$  of dimensions  $d \times n$  and  $d$ -dimensional bias vector  $\mathbf{b}$ .

A trained network is used for time series prediction recursively. Namely, one starts with a sequence  $\mathbf{X}^1 = \mathbf{X}_{k,m}$  of length  $m$  supplied as input to the RNN; the resulting output is considered as a prediction of the next time point  $\bar{\mathbf{x}}_{k+m+1}$  of the input sequence. The next input sequence  $\mathbf{X}^2$  to RNN is produced by dropping the first point of  $\mathbf{X}^1$  and adding the predicted point to the result:  $\mathbf{X}^2 = \mathbf{X}_{k+1,m-1} \cup \bar{\mathbf{X}}_{k+m,1}$ ; here  $\cup$  denotes union of two sequences with order of elements preserved. This sequence is used as input to the RNN that generates  $\bar{\mathbf{x}}_{k+m+2}$  and a next input  $\mathbf{X}^3 = \mathbf{X}_{k+2,m-2} \cup \bar{\mathbf{X}}_{k+m,2}$  is formed. Thus at  $j$ -th predictive step ( $j \leq m$ ) the input  $\mathbf{X}_k^j$  to RNN is formed as  $\mathbf{X}^j = \mathbf{X}_{k+j-1,m-j+1} \cup \bar{\mathbf{X}}_{k+m,j-1}$ , while for  $j > m$  the input is formed by the already predicted values only  $\mathbf{X}^j = \bar{\mathbf{X}}_{k+j-m-1,m}$ . The recursive procedure is repeated  $p$  times to produce  $p$  new time points  $\bar{\mathbf{x}}_{k+m+i}$ , ( $1 \leq i \leq p$ ) approximating the time series  $\mathbf{X}$  segment  $\{\mathbf{x}_i\}$  for  $k+m+1 \leq i \leq k+m+p$  (Figure 1). It is easy to see that the described predictive procedure uses a double recursion – the inner one used  $m$  times in the recurrent layer and the outer is employed  $p$  times to generate the output points, so that the total number of recursions is  $mp$ . During the network training the minimization of a scalar loss function

$$L = \sum_{i=1}^p (\bar{\mathbf{x}}_{k+m+i} - \mathbf{x}_{k+m+i})^2,$$

leads to determination of the trainable components of the network. As the offset value  $k$  determining the initial point of the input sequence  $\mathbf{X}^1$  is arbitrary but fixed for given predictive procedure, without loss of generality we further set it equal to zero.

## 3 State vector dynamics governing equations

In this manuscript we restrict the analysis to recurrent layers of two types – basic recurrent network and LSTM network [7], but it can be extended to any recurrent layer. Consider a performance of a recurrent layer in more details. The input sequence  $\mathbf{X} = \{\mathbf{x}_i\}$ ,  $1 \leq i \leq m$  produces the network state  $\mathbf{S} = \{\mathbf{s}_i\}$  sequence for the basic network

$$\mathbf{s}_i = \tanh(\mathbf{W}_x \cdot \mathbf{x}_i + \mathbf{W}_s \cdot \mathbf{s}_{i-1} + \mathbf{b}_s), \quad (1)$$

where  $\mathbf{W}_x$ ,  $\mathbf{W}_s$  are matrices and  $\mathbf{b}_s$  is a bias vector. For LSTM network the governing transformation that determines network state  $\mathbf{S} = \{\mathbf{s}_i\}$  and cell state  $\mathbf{C} = \{\mathbf{c}_i\}$  sequences is defined by

$$\begin{aligned} \mathbf{s}_i &= \mathbf{o}_i \otimes \tanh \mathbf{c}_i, \\ \mathbf{c}_i &= \mathbf{f}_i \otimes \mathbf{c}_{i-1} + \mathbf{i}_i \otimes \mathbf{m}_i, \\ \mathbf{o}_i &= \sigma(\mathbf{W}_{ox}\mathbf{x}_i + \mathbf{W}_{os}\mathbf{s}_{i-1} + \mathbf{b}_o), \\ \mathbf{i}_i &= \sigma(\mathbf{W}_{ix}\mathbf{x}_i + \mathbf{W}_{is}\mathbf{s}_{i-1} + \mathbf{b}_i), \\ \mathbf{f}_i &= \sigma(\mathbf{W}_{fx}\mathbf{x}_i + \mathbf{W}_{fs}\mathbf{s}_{i-1} + \mathbf{b}_f), \\ \mathbf{m}_i &= \tanh(\mathbf{W}_{mx}\mathbf{x}_i + \mathbf{W}_{ms}\mathbf{s}_{i-1} + \mathbf{b}_m), \end{aligned} \tag{2}$$

where  $\sigma(x) = 1/(1 + \exp(-x))$  is the logistic sigmoid function and the initialization value of state  $\mathbf{s}_0$  and cell state  $\mathbf{c}_0$  vector is zero vector of length  $n$ , and  $\otimes$  denotes elementwise multiplication. With  $a = i, f, m, o$  we denote  $\mathbf{W}_{ax}$ ,  $\mathbf{W}_{as}$  matrices and  $\mathbf{b}_a$  bias vectors for the input, forget, memory and output gates respectively; all these structures are trainable and in the trained network their elements are real valued constants.

The shorthand form of the transformations (1,2) reads

$$\mathbf{s}_i = \mathcal{F}(\mathbf{x}_i, \mathbf{s}_{i-1}, \mathbf{P}). \tag{3}$$

where  $\mathbf{P}$  denotes elements of all matrices and bias vectors in (1,2) and  $\mathbf{s}_0$  is  $n$ -dimensional zero vector. As the set  $\mathbf{P}$  is fixed we will drop it from the list of arguments of the vector function  $\mathcal{F}$

$$\mathbf{s}_i = \mathcal{F}(\mathbf{x}_i, \mathbf{s}_{i-1}), \quad \mathcal{F}: R^{d \times n} \rightarrow R^n. \tag{4}$$

It is important to note that the governing transformations imply for every step  $i$  in (4) all components of  $\mathbf{s}$  satisfy a condition  $|s_k| \leq 1, 1 \leq k \leq n$ . The equations (1,2) are accompanied by a linear transformation

$$\bar{\mathbf{x}}_{m+1} = \mathbf{W} \cdot \mathbf{s}_m + \mathbf{b}, \tag{5}$$

where  $\bar{\mathbf{x}}_{m+1}$  is a value predicted by RNN based on the input  $\mathbf{X}$ .

## 4 RNN training and performance

The RNNs we use in the simulation have a small number  $n$  of neurons in the recurrent layer  $1 \leq n \leq 20$ . The training set is constructed by merging 6000 segments of variable length ( $5 \leq m \leq 150$ ) of two periodic one-dimensional ( $d = 1$ ) functions – the sine wave  $g_0(t) = \sin(2\pi t)$  and the shifted triangle wave  $h_0(t) = 1/2 + 1/\pi \arcsin(\sin 2\pi x)$ . The white noise with the amplitude  $a = 0.15$  is added to both functions –  $g(t) = g_0(t) + a\xi(t)$ ,  $h(t) = h_0(t) + a\xi(t)$ . The time step  $\Delta t$  between the adjacent time points is selected equal to  $\Delta t = 0.01$ . The RNNs are trained for 50 epochs on the complete set of 12000 segments with 20% validation set using Adam algorithm. The RNNs fail to predict the noisy dynamics of  $g(t)$  or  $h(t)$ , instead all RNNs produce some smooth predictions  $G_0(t)$  and  $H_0(t)$ , respectively. We define the quality function of prediction  $F(t)$  vs. the actual dynamics  $f(t)$  ( $f = g, h$  and  $F = G, H$ ) as

$$Q^{-1} = \frac{1}{p} \sum_{i=1}^p \|F(t_i) - f(t_i)\|^2,$$

where  $p$  is the length of the predicted sequence and  $\| \cdot \|$  denotes the Euclidean norm.

As it was expected the value of  $Q$  for the LSTM network increases with  $n$  (see Figure 2). Nevertheless the predicted dynamics is always smooth which implies that the filtering property of RNN is independent of the prediction quality. We observe that for  $n = 10$  the deviation of the predicted curve from the actual one is quite small for one period ( $Q > 30$ ). Note that the prediction of the underlying smooth function was very good for  $n = 20$  neurons ( $Q > 100$ ) which is much smaller than ( $n = 128$ ) reported in [6]. Qualitatively similar results are obtained for the basic recurrent network.

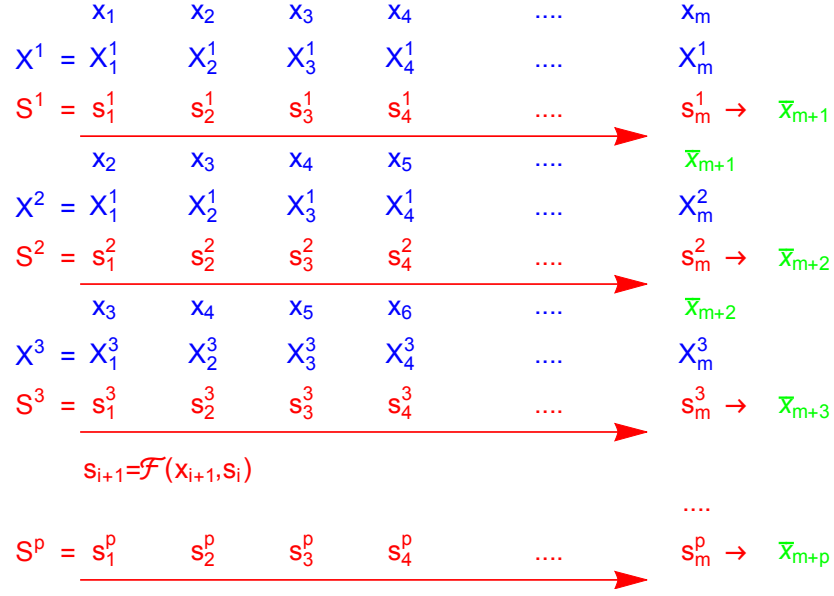


Figure 1: The scheme of the prediction double recursive procedure for RNN. Three first and the last prediction steps are shown. The elements of the input sequences  $\mathbf{X}^j$  to RNN (blue) are fed into (4) to produce recursively recurrent network states  $\mathbf{s}_i^j$  (red). The last element  $\mathbf{s}_m^j$  in  $\mathbf{S}^j$  is transformed by (5) to generate the predicted point  $\bar{\mathbf{x}}_{m+j+1}$  (shown in green). This point is used to update the input sequence  $\mathbf{X}^{j+1}$  for the next prediction step.

## 5 Noise propagation in recurrent network

Consider the process of state vector computation assuming that the input sequence  $\mathbf{X}$  represents time point values of the function  $\mathbf{g}(t) = \mathbf{g}_0(t) + a\boldsymbol{\xi}(t)$  where  $\mathbf{g}_0(t)$  is a smooth function,  $\boldsymbol{\xi}$  is a white noise random process with a small amplitude  $0 \leq a \ll 1$ . This implies that RNN is trained to predict the values  $\mathbf{x}_i = \mathbf{g}_0(t_i) + a\boldsymbol{\xi}(t_i)$  for  $i > m$  using the input  $\mathbf{X}_m$ . As the parameters  $\mathbf{P}$  of the transformation (3) are constants one expects that the values  $\mathbf{s}_i$  for  $i > 0$  might contain a noisy component and that eventually a sequence  $\bar{\mathbf{X}}_{m,p}$  of the predicted values would be a representation of some noisy function. In other words, RNN is expected to produce a discrete representation of a function  $\mathbf{G}(t)$  that mimics with some accuracy the *noisy* function  $\mathbf{g}(t)$  using the *noisy* input  $\mathbf{X}_m$  representing the same function  $\mathbf{g}(t)$ .

Consider step by step computation of  $\mathbf{s}_i$ . Using smallness of the noise amplitude  $a$  we find for  $\mathbf{s}_1$  from (4) using Taylor expansion in  $a$  in linear approximation

$$\mathbf{s}_1 = \mathcal{F}(\mathbf{g}_0(t_1) + a\boldsymbol{\xi}_1, \mathbf{0}) \approx \mathcal{F}(\mathbf{g}_0(t_1), \mathbf{0}) + a\mathcal{F}'(\mathbf{g}_0(t_1), \mathbf{0}) \otimes \boldsymbol{\eta}_1 = \hat{\mathbf{s}}_1 + a\tilde{\mathbf{s}}_1 \otimes \boldsymbol{\eta}_1, \quad (6)$$

where  $\boldsymbol{\eta}$  is a  $n$ -dimensional random process obtained by a linear transformation of the  $d$ -dimensional random process  $\boldsymbol{\xi}$ . The computation of  $\mathbf{s}_2$  gives

$$\begin{aligned} \mathbf{s}_2 &= \mathcal{F}(\mathbf{g}_0(t_2) + a\boldsymbol{\xi}_2, \hat{\mathbf{s}}_1 + a\tilde{\mathbf{s}}_1 \otimes \boldsymbol{\eta}_1) \\ &\approx \mathcal{F}(\mathbf{g}_0(t_2), \hat{\mathbf{s}}_1) + a\mathcal{F}'(\mathbf{g}_0(t_2), \hat{\mathbf{s}}_1) \otimes (\boldsymbol{\eta}_2 + \bar{\mathbf{W}} \cdot \tilde{\mathbf{s}}_1 \otimes \boldsymbol{\eta}_1) \\ &= \mathcal{F}(\mathbf{g}_0(t_2), \hat{\mathbf{s}}_1) + a\mathcal{F}'(\mathbf{g}_0(t_2), \hat{\mathbf{s}}_1) \otimes \boldsymbol{\zeta}_2 = \hat{\mathbf{s}}_2 + a\tilde{\mathbf{s}}_2 \otimes \boldsymbol{\zeta}_2, \\ \boldsymbol{\zeta}_2 &= \boldsymbol{\eta}_2 + \bar{\mathbf{W}} \cdot \tilde{\mathbf{s}}_1 \otimes \boldsymbol{\eta}_1, \end{aligned} \quad (7)$$

where  $\bar{\mathbf{W}}$  denotes a matrix used in transformation of the noise component generated in the vector  $\mathbf{s}_1$ .

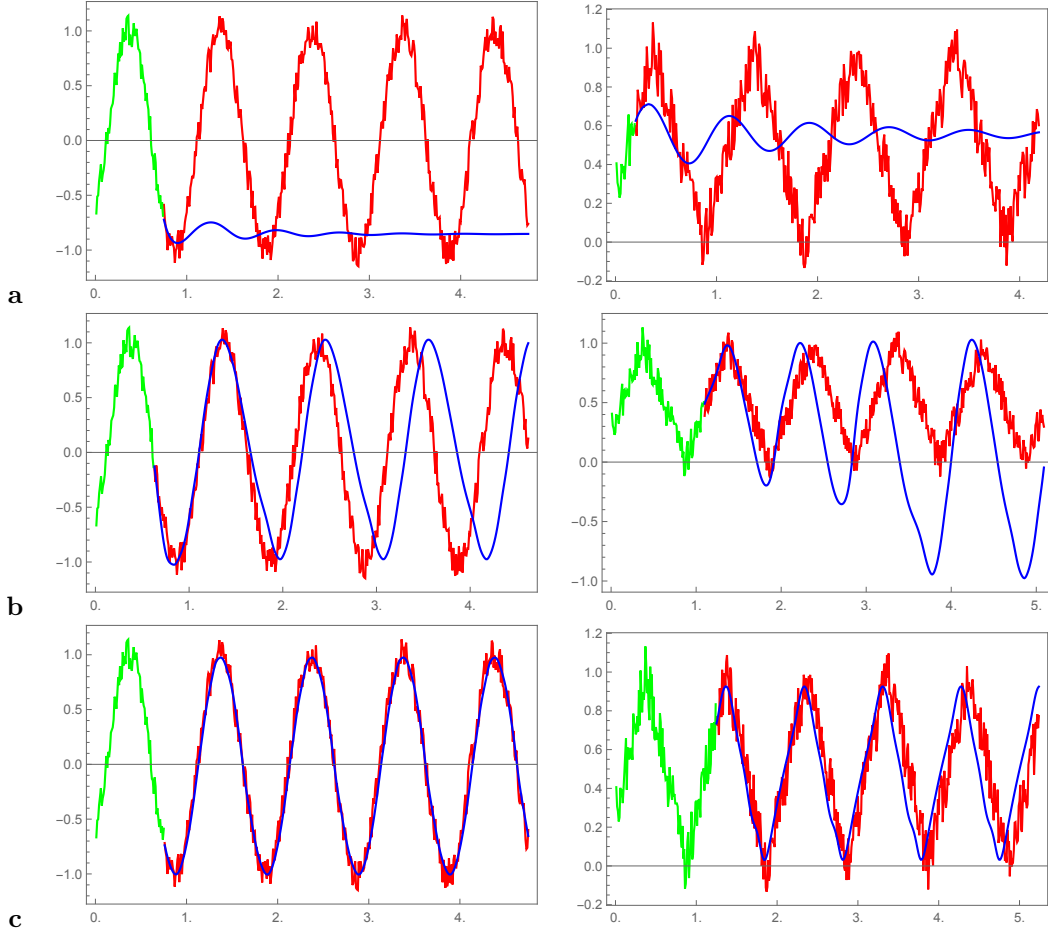


Figure 2: The input segment of the noisy ( $a = 0.15$ ) sequence (green) of sine (left) and triangular (right) waves, the subsequent segment of  $\mathcal{X}$  (red) and predicted dynamics (blue) for (a) 5, (b) 10, (c) 20 neurons in LSTM network.

The subsequent steps ( $1 \leq k \leq m$ ) produce

$$\begin{aligned}
s_k &= \mathcal{F}(g_0(t_k) + a\xi_k, \hat{s}_{k-1} + a\bar{s}_{k-1} \otimes \zeta_{k-1}) \\
&\approx \mathcal{F}(g_0(t_k), \hat{s}_{k-1}) + a\mathcal{F}'(g_0(t_k), \hat{s}_{k-1}) \otimes (\eta_k + \bar{W} \cdot \tilde{s}_{k-1} \otimes \zeta_{k-1}) \\
&= \mathcal{F}(g_0(t_k), \hat{s}_{k-1}) + a\mathcal{F}'(g_0(t_k), \hat{s}_{k-1}) \otimes \zeta_k = \hat{s}_k + a\tilde{s}_k \otimes \zeta_k, \\
\zeta_k &= \eta_k + \bar{W} \cdot \tilde{s}_{k-1} \otimes \zeta_{k-1},
\end{aligned} \tag{8}$$

where

$$\hat{s}_k = \mathcal{F}(g_0(t_k), \hat{s}_{k-1}), \quad \tilde{s}_k = \mathcal{F}'(g_0(t_k), \hat{s}_{k-1}),$$

and the derivative is taken w.r.t. noise amplitude  $a$ . Note that (8) is valid for  $k = 1, 2$  if one defines  $\zeta_1 = \eta_1 + \tilde{s}_0 \otimes \zeta_0$ , and  $\tilde{s}_0$  as zero vector.

From (8) it follows that the last element  $s_m$  of the state sequence also has the noise contribution  $a\tilde{s}_m \otimes \zeta_m$  which naturally transfers to the first predicted value

$$\bar{x}_{m+1} = W \cdot \hat{s}_m + b + aW \cdot \tilde{s}_m \otimes \zeta_m = G(t_{m+1}) = G_0(t_{m+1}) + aW \cdot \tilde{s}_m \otimes \zeta_m,$$

where  $G$  and  $G_0$  are approximations to the functions  $g$  and  $g_0$  generated by RNN. This means that the RNN by itself only transforms the input noise but cannot filter it out.

The predicted element  $\bar{x}_{m+1}$  is used as the last element of the input sequence in the next prediction step and therefore one expects that the predicted sequence  $\bar{\mathbf{X}}_{m,p}$  should reflect the noise components contained both in the input and predicted sequences. Unexpectedly, the numerical experiments (see below) show that in fact the predicted sequence  $\bar{\mathbf{X}}_{m,p}$  is not noisy but represents the approximation  $\mathbf{G}_0(t)$  of the smooth function  $\mathbf{g}_0(t)$ . The goal of this manuscript is to explain this unexpected behavior and to determine conditions required for generation of a smooth prediction.

## 6 RNN state dynamics

In the previous Section we observe that the noise component of the input signal is preserved in the RNN states, and we have to look at state dynamics in more details to understand noise filtering in the trajectory prediction process.

### 6.1 Numerical experiments

We focus on the case  $n = 10$  as for this number of neurons the smoothness of the prediction is accompanied by a quite high prediction quality of the underlying smooth dynamics. We consider in details the sequence of the RNN states  $\mathbf{S}^1$  and  $\mathbf{S}^2$  for zeroth and first prediction steps for three values of the noise amplitude  $a = 0, 0.15, 0.9$  of the input sequence. Figure 3a demonstrates that indeed the dynamics of LSTM state is affected by noise as predicted by (8). We also note that both sequences  $\mathbf{S}^1$  and  $\mathbf{S}^2$  look very similar. To test this similarity we overlay the corresponding sequences for given noise amplitude (Figure 3b-d) and find that even in case of large noise  $a = 0.9$  the sequence  $\mathbf{S}^2$  is very close to the sequence  $\mathbf{S}^1$  shifted by one step to the left, in other words  $\mathbf{s}_i^2 \approx \mathbf{s}_{i+1}^1$ .

### 6.2 Dynamics of state vector shifted difference

To understand this behavior recall a relation between the input sequences  $\mathbf{X}^j$  and  $\mathbf{X}^{j+1}$  (see Figure 1). The input sequence  $\mathbf{X}^j$  construction algorithm described in Section 3 implies that  $\mathbf{X}_i^{j+1} = \mathbf{X}_{i+1}^j$  for all  $2 \leq i \leq m-1$ . Using (4) we find

$$\mathbf{s}_{i+1}^1 = \mathcal{F}(\mathbf{X}_{i+1}^1, \mathbf{s}_i^1), \quad 0 \leq i \leq m-1, \quad (9)$$

$$\mathbf{s}_i^2 = \mathcal{F}(\mathbf{X}_i^2, \mathbf{s}_{i-1}^2) = \mathcal{F}(\mathbf{X}_{i+1}^1, \mathbf{s}_{i-1}^2), \quad 1 \leq i \leq m-1. \quad (10)$$

We observe that in computation of  $\mathbf{s}_{i+1}^1$  and  $\mathbf{s}_i^2$  the first argument of the map  $\mathcal{F}$  in (9,10) is the same. Consider the difference  $\delta_i^1 = \mathbf{s}_{i+1}^1 - \mathbf{s}_i^2$ . For  $i = 0$  we have  $\delta_1^1 = \mathbf{s}_1^1 = \mathcal{F}(\mathbf{X}_1^1, \mathbf{0})$ . For  $i = 1$  find

$$\delta_1^1 = \mathbf{s}_2^1 - \mathbf{s}_1^2 = \mathcal{F}(\mathbf{X}_2^1, \mathbf{s}_1^1) - \mathcal{F}(\mathbf{X}_2^1, \mathbf{0}) = \mathcal{F}(\mathbf{X}_2^1, \delta_0^1) - \mathcal{F}(\mathbf{X}_2^1, \mathbf{0}).$$

Assuming  $\|\delta_0^1\| \ll 1$  expand the first term above and retain the leading order to obtain

$$\delta_1^1 = \frac{\partial \mathcal{F}(\mathbf{X}_2^1, \mathbf{s} = \mathbf{0})}{\partial \mathbf{s}} \cdot \delta_0^1 = \mathbf{A}_1^1 \cdot \delta_0^1. \quad (11)$$

With  $i = 2$  find

$$\delta_2^1 = \mathbf{s}_3^1 - \mathbf{s}_2^2 = \mathcal{F}(\mathbf{X}_3^1, \mathbf{s}_2^1) - \mathcal{F}(\mathbf{X}_3^1, \mathbf{s}_1^2) = \mathcal{F}(\mathbf{X}_3^1, \mathbf{s}_2^1 + \delta_1^1) - \mathcal{F}(\mathbf{X}_3^1, \mathbf{s}_1^2),$$

and the expansion leads to

$$\delta_2^1 = \frac{\partial \mathcal{F}(\mathbf{X}_3^1, \mathbf{s} = \mathbf{s}_1^2)}{\partial \mathbf{s}} \cdot \delta_1^1 = \mathbf{A}_2^1 \cdot \delta_1^1 = \mathbf{A}_1^1 \cdot \mathbf{A}_2^1 \cdot \delta_0^1. \quad (12)$$

It is easy to deduce that for  $i = m$

$$\delta_m^1 = \mathbf{A}^1 \cdot \delta_0^1, \quad \mathbf{A}^1 = \prod_{k=0}^{m-1} \mathbf{A}_k^1, \quad \mathbf{A}_k^1 = \frac{\partial \mathcal{F}(\mathbf{X}_{k+1}^1, \mathbf{s} = \mathbf{s}_{k-1}^2)}{\partial \mathbf{s}}. \quad (13)$$

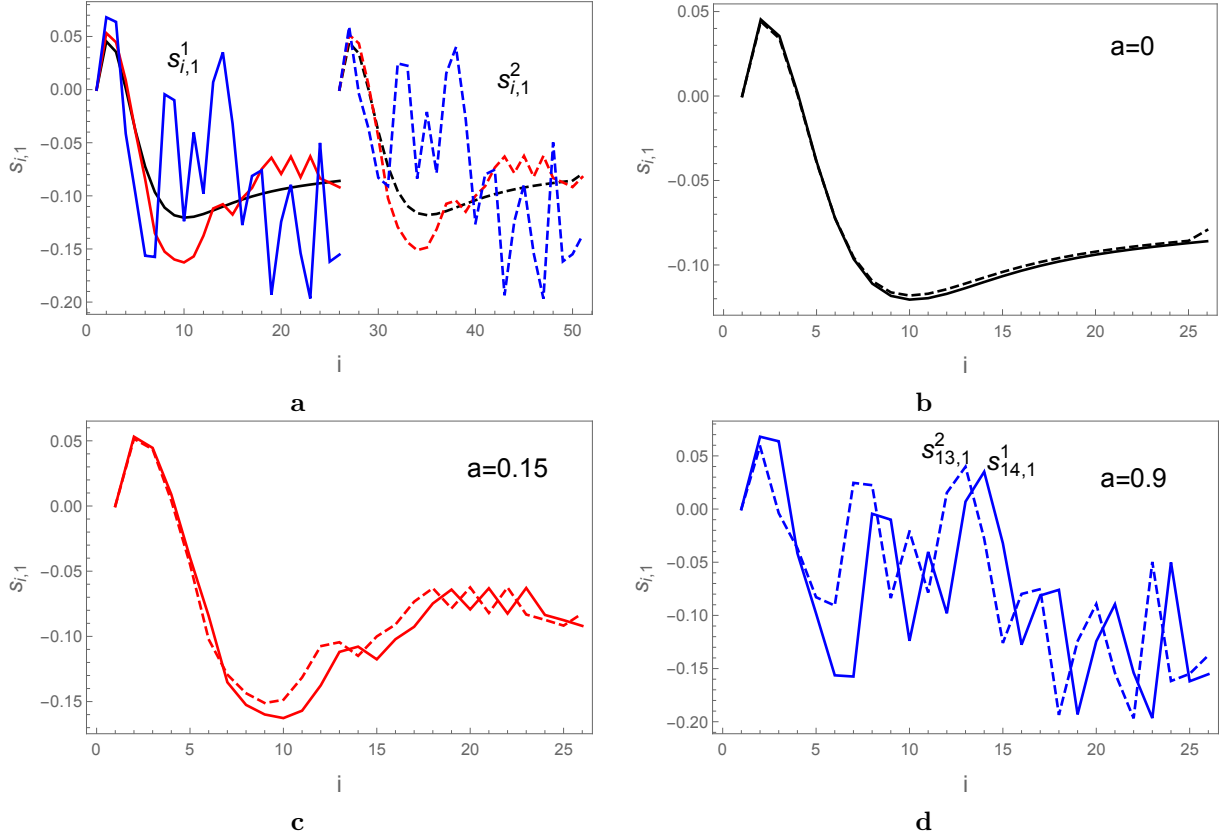


Figure 3: The dynamics of the first element  $s_{i,1}^j$  of the state vector  $\mathbf{s}_i^j$  in the  $j$ -th round of prediction for  $j = 1$  (solid) and  $j = 2$  (dashed) for three noise amplitudes –  $a = 0$  (black),  $a = 0.15$  (red) and  $a = 0.9$  (blue). (a) The sequence  $s_{i,1}^2$  is shifted w.r.t. of  $s_{i,1}^1$ . (b - d) The sequences are overlapped for different noise amplitudes: (b)  $a = 0$  (no noise), (c) original amplitude  $a = 0.15$ , (d) increased amplitude  $a = 0.9$ . The values of  $s_{i+1,1}^1$  and  $s_{i,1}^2$  tend to each other with increasing  $i$ .

Generalizing the above relations to the other rounds of the predictive cycle we obtain for  $\delta_i^j = \mathbf{s}_{i+1}^j - \mathbf{s}_i^{j+1}$ :

$$\delta_m^j = \mathbf{A}^j \cdot \delta_0^j, \quad \mathbf{A}^j = \prod_{k=0}^{m-1} \mathbf{A}_k^j, \quad 1 \leq j \leq p. \quad (14)$$

If  $\det \mathbf{A}_i^j < 0$  (contracting transformation) a deviation norm  $\delta_i^j = \|\delta_i^j\|$  satisfies  $\delta_i^j < \delta_{i-1}^j$  and decays exponentially. For basic RNN it is possible to find an explicit expression for the elements of matrix  $\mathbf{A}_i^j$  and the simulations show that indeed  $\det \mathbf{A}_i^j < 0$ . We thus confirm the assumption on the exponential decay of difference norm of state vectors (Figure 4).

In the LSTM network the relations similar to (9-14) are valid with respect to the cell state vectors  $\mathbf{c}_i^j$  and one can write for  $\mathbf{d}_i^j = \mathbf{c}_{i+1}^j - \mathbf{c}_i^{j+1}$ :

$$\mathbf{d}_m^j = \mathbf{B}^j \cdot \mathbf{d}_0^j, \quad \mathbf{B}^j = \prod_{k=0}^{m-1} \mathbf{B}_k^j, \quad \mathbf{B}_k^j = \frac{\partial \mathcal{F}(\mathbf{X}_{k+1}^j, \mathbf{c} = \mathbf{c}_{k-1}^{j+1})}{\partial \mathbf{c}}, \quad 1 \leq j \leq p. \quad (15)$$

Similarly, with  $\det \mathbf{B}_i^j < 0$ , a deviation norm  $d_i^j = \|\mathbf{d}_i^j\|$  satisfies  $d_i^j < d_{i-1}^j$  and would decrease exponentially. The computations for  $j = 1$  show (see Figure 5) that indeed both  $\delta_i^1$  and  $d_i^1$  decrease exponentially with  $i$

$$\delta_i^1 = \delta_1^1 e^{-\alpha i}, \quad d_i^1 = d_1^1 e^{-\beta i}, \quad (16)$$

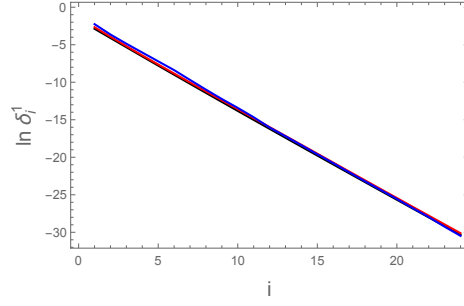


Figure 4: In the basic RNN with  $n = 10$  neurons the difference norm for state vectors  $\delta_i^1$  decays exponentially with  $i$  for the noise amplitude  $a = 0$  (black), 0.15 (red) and 0.9 (blue).

and both decay rates  $\alpha$  and  $\beta$  are not affected by the noise strength but depend on  $i$ , i.e., for large  $i$  they might tend to zero. It is possible that decay rates behavior depends on the number of neurons  $n$ . The simulations show that similar behavior remains valid for all steps of the prediction procedure

$$\delta_i^j \sim e^{-\alpha i}, \quad d_i^j \sim e^{-\beta i}, \quad 1 \leq j \leq p. \quad (17)$$

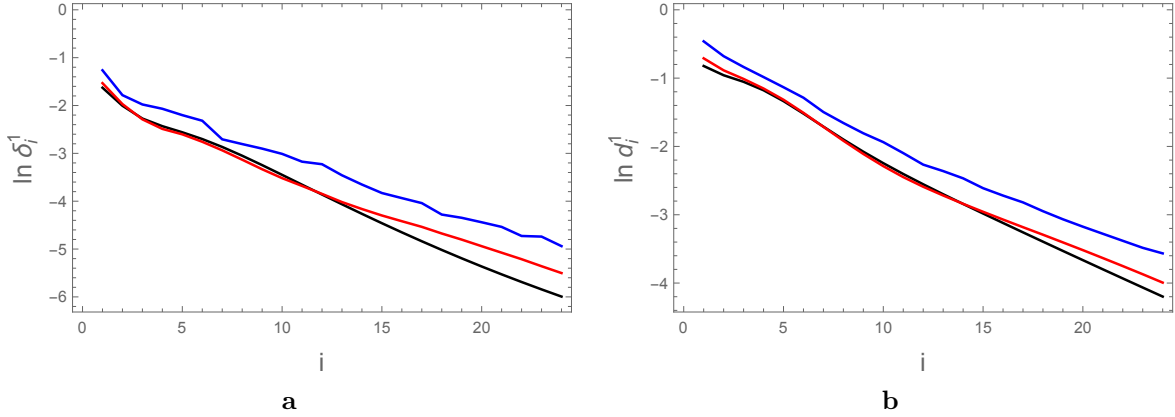


Figure 5: The difference norms (a)  $\delta_i^1$  of state vectors and (b)  $d_i^1$  of cell vectors of LSTM network decay exponentially with  $i$  for the noise amplitude  $a = 0$  (black), 0.15 (red) and 0.9 (blue).

This means also that the state vector  $\mathbf{s}_{m-1}^{j+1}$  (next to last in the sequence  $\mathbf{S}^{j+1}$ ) is very close to the last vector  $\mathbf{s}_m^j$  of the preceding sequence  $\mathbf{S}^j$ , i.e.,

$$\mathbf{s}_{m-1}^{j+1} = \mathbf{s}_m^j + \boldsymbol{\epsilon}^j, \quad \|\boldsymbol{\epsilon}^j\| \ll 1. \quad (18)$$

### 6.3 Approximate governing transformation

Now it is time to recall that the state vector  $\mathbf{s}_m^j$  gives rise to the prediction  $\bar{\mathbf{x}}_{m+j} = \mathbf{W} \cdot \mathbf{s}_m^j + \mathbf{b}$ , and this value is used as the last element of the input sequence for the next prediction step:  $\mathbf{X}_m^{j+1} = \mathbf{W} \cdot \mathbf{s}_m^j + \mathbf{b}$ .

Employ the relation (4) for  $i = m$  to find

$$\mathbf{s}_m^{j+1} = \mathcal{F}(\mathbf{X}_m^{j+1}, \mathbf{s}_{m-1}^{j+1}) = \mathcal{F}(\mathbf{W} \cdot \mathbf{s}_m^j + \mathbf{b}, \mathbf{s}_m^j + \boldsymbol{\epsilon}^j) \approx \mathcal{F}(\mathbf{W} \cdot \mathbf{s}_m^j + \mathbf{b}, \mathbf{s}_m^j) = \mathcal{G}(\mathbf{s}_m^j). \quad (19)$$



The map  $\mathcal{G}$  for LSTM is defined by the transformations

$$\begin{aligned} \mathbf{s}_m^j &= \mathbf{o}_m^j \otimes \tanh \mathbf{c}_m^j, & \mathbf{c}_m^j &= \mathbf{f}_m^j \otimes \mathbf{c}_m^{j-1} + \mathbf{i}_m^j \otimes \mathbf{m}_m^j, \\ \mathbf{o}_m^j &= \sigma(\tilde{\mathbf{W}}_{os} \mathbf{s}_m^{j-1} + \tilde{\mathbf{b}}_o), & \mathbf{i}_m^j &= \sigma(\tilde{\mathbf{W}}_{is} \mathbf{s}_m^{j-1} + \tilde{\mathbf{b}}_i), \\ \mathbf{f}_m^j &= \sigma(\tilde{\mathbf{W}}_{fs} \mathbf{s}_m^{j-1} + \tilde{\mathbf{b}}_f), & \mathbf{m}_m^j &= \tanh(\tilde{\mathbf{W}}_{ms} \mathbf{s}_m^{j-1} + \tilde{\mathbf{b}}_m), \end{aligned} \quad (20)$$

where

$$\tilde{\mathbf{W}}_{as} = \mathbf{W}_{ax} \cdot \mathbf{W} + \mathbf{W}_{as}, \quad \tilde{\mathbf{b}}_a = \mathbf{W}_{ax} \cdot \mathbf{b} + \mathbf{b}_a, \quad a = i, f, m, o, \quad (21)$$

and  $\mathbf{s}_m^0$  and  $\mathbf{c}_m^0$  are obtained by application of (2) to the original input sequence. Similarly for basic RNN we find

$$\begin{aligned} \mathbf{s}_m^j &= \tanh(\mathbf{W}_x \cdot (\mathbf{W} \cdot \mathbf{s}_m^{j-1} + \mathbf{b}) + \mathbf{W}_s \cdot \mathbf{s}_m^{j-1} + \mathbf{b}_s) \\ &= \tanh([\mathbf{W}_x \cdot \mathbf{W} + \mathbf{W}_s] \cdot \mathbf{s}_m^{j-1} + \mathbf{W}_x \cdot \mathbf{b} + \mathbf{b}_s) = \tanh(\tilde{\mathbf{W}}_s \cdot \mathbf{s}_m^{j-1} + \tilde{\mathbf{b}}_s), \end{aligned} \quad (22)$$

with

$$\tilde{\mathbf{W}}_s = \mathbf{W}_x \cdot \mathbf{W} + \mathbf{W}_s, \quad \tilde{\mathbf{b}}_s = \mathbf{W}_x \cdot \mathbf{b} + \mathbf{b}_s. \quad (23)$$

We observe that the influence of the input sequence  $\mathbf{X}^j$  (and the noise contained in it) on the the dynamics of the RNN last state vector  $\mathbf{s}_m^j$  is negligible and the latter is almost completely determined by the same vector  $\mathbf{s}_m^{j-1}$  at the preceding prediction step.

Finally, the linear transformation (5) allows to rewrite (19) as a recursion for the predicted points

$$\bar{\mathbf{x}}_{m+j+1} = \mathbf{W} \cdot \mathcal{G}(\mathbf{W}^{-1} \cdot (\bar{\mathbf{x}}_{m+j} - \mathbf{b})) + \mathbf{b} = \bar{\mathcal{G}}(\bar{\mathbf{x}}_{m+j}). \quad (24)$$

## 7 A new fast algorithm for trajectory prediction

The main result in previous Section implies that after computation of  $\mathbf{s}_m^1$  using  $m$  times the recursion (4) the original input sequence can be dropped and (19) is applied recursively  $p-1$  times to generate  $\mathbf{s}_m^j$  for  $2 \leq j \leq p$ . Then the linear transformation (5) produces the desired sequence  $\bar{\mathbf{x}}_{m+j}$  for  $1 \leq j \leq p$ .

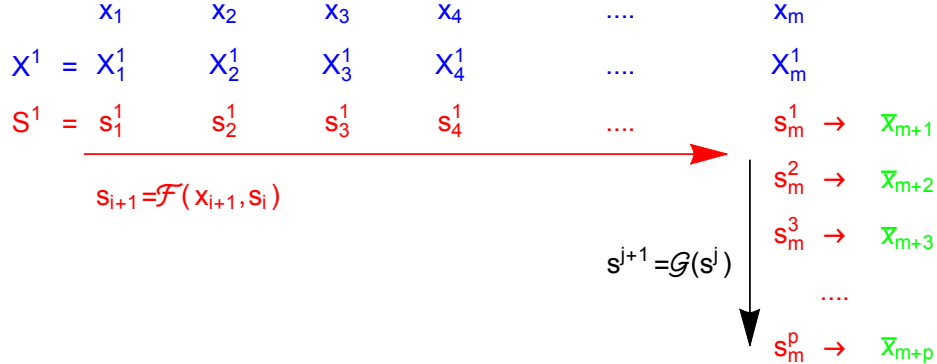


Figure 6: The approximate scheme of the recursive prediction based on (19). The standard prediction sequence (4) is evoked only once to produce  $\mathbf{s}_m^1$  and then the approximate algorithm (19) is applied recursively to produce  $\mathbf{s}_m^j$  (red). The predicted points  $\bar{\mathbf{x}}_{m+j}$  (green) are computed using (5).

These steps represent a new very fast prediction algorithm (Figure 6). The transformation (19) might produce in principle non-smooth and even chaotic dynamics but nevertheless it is important that the noise component in the input sequence plays no role in the generation of the anticipated points. On the other hand this noise component can strongly affect the result of RNN training influencing the weights and biases of the trained network.

We use the approximate map (19) to compute the predicted sequence for the input of different length  $m$  and compare the results to the prediction made by iterative application of RNN. We find that increase in

input sequence length  $m$  improves the approximate prediction (Figure 7) up to a perfect coincidence with the traditional approach prediction. It is explained by the fact that for large  $m$  the difference  $\epsilon^1$  becomes extremely small that increases the accuracy of the map (19). Moreover, when we increase the input sequence noise amplitude  $a$  six times compared to the value at which LSTM network was trained, the approximate procedure still generates prediction coinciding with the one produced by LSTM itself (Figure 7d).

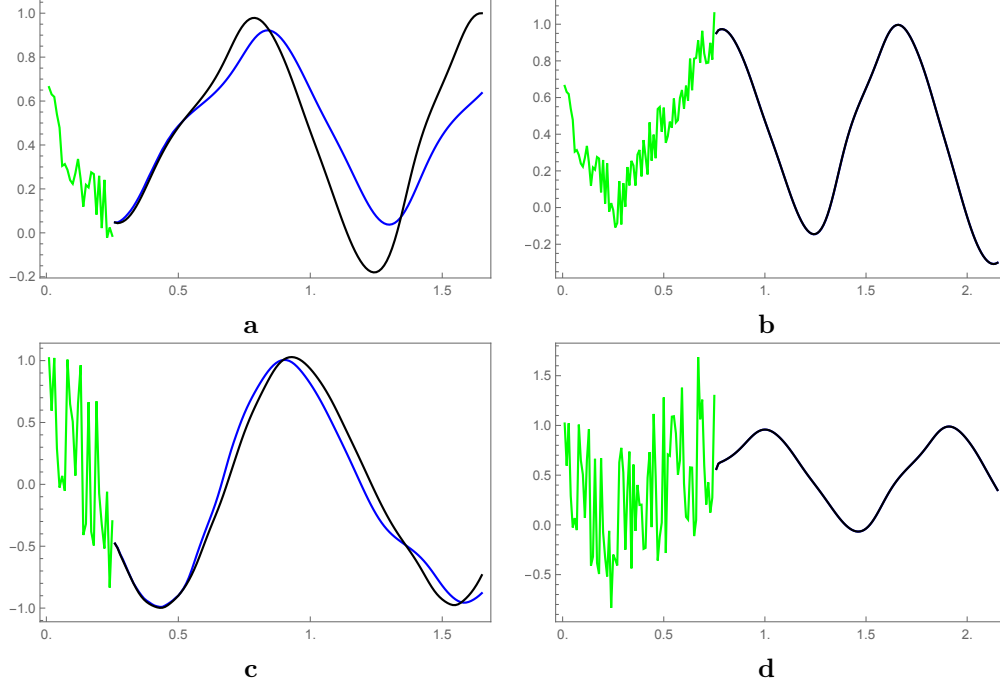


Figure 7: Comparison of the predictions by the trained LSTM network (blue) and by using the map (19) (black) for the triangle wave input sequence (green) with variable noise amplitude  $a$  and length  $m$ : (a)  $a = 0.15$ ,  $m = 25$ , (b)  $a = 0.15$ ,  $m = 75$ , (c)  $a = 0.9$ ,  $m = 25$ , (d)  $a = 0.9$ ,  $m = 75$ ; in (b) and (d) both predictions coincide.

We also compare the predictions made by the RNN governed by (1) and (22) and find that these predictions coincide for large  $m$  (Figure 8b).

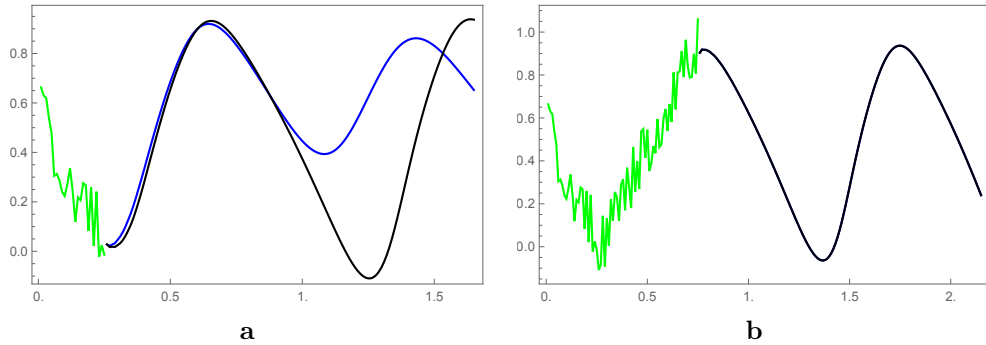


Figure 8: Comparison of the predictions by the basic RNN (blue) with  $n = 10$  and by the map (22) (black) for the triangle wave input sequence (green) of (a)  $m = 25$  and (b)  $m = 75$  points with noise amplitude  $a = 0.15$ ; in (b) both predictions coincide.

We observe that the original prediction procedure of  $p$  time series points using the trained RNN is a

recursion ( $p$  times) each consisting of  $m$  inner recursions, i.e., total  $R_o = mp$  recursions while the approximate procedure (19) replaces it by  $R_a = m + p - 1$  recursions (Figure 6). Assuming that the computation time  $\mathcal{T}$  is linearly proportional to the total recursion number  $\mathcal{T} = \mu R$  estimate a speed up  $\kappa = \mathcal{T}_o/\mathcal{T}_a$ . The length  $m$  of the input sequence  $\mathbf{X}$  should be quite large ( $m \gg 1$ ) in order to generate a high quality prediction. The length  $p = \gamma m$  of the predicted sequence  $\bar{\mathbf{X}}$  is comparable to  $m$ , i.e.,  $\gamma \gtrsim 1$  and we find the estimate of the prediction times ratio  $\kappa = mp/(m+p) = \gamma m/(1+\gamma) > m/2$ . Thus the approximate prediction algorithm gain is proportional to the length of the input sequence. We observed that  $m \approx 100$  leads to very good quality of the approximate scheme (Figures 7, 8) and thus one can have speed up of a two orders of magnitude without loss of prediction quality.

## 8 Discussion

In this manuscript we show that the predictive RNN based on a single recurrent layer with a small number of neurons works as an effective noise filter. Namely, when the RNN is supplied by the noisy input sequence of (multidimensional) time series points and used recursively for series extrapolation it generates points that belong to some smooth curve that mimics the smoothed original time series. Using the analysis of the recursive prediction procedure we established a set of conditions required to observe such behavior. These conditions imply that the governing transformation of the predictive algorithm reduces to one that requires the input sequence only once and later does not depend on it. As the result the predictive algorithm can be drastically simplified and accelerated without loss of accuracy. The overall quality of prediction strongly depends on the length of the input sequence while the acceleration is proportional to it. Thus using the approximate predictive algorithm one can both increase the quality and save time and computational resources.

These results allow to deduce that RNNs with several recurrent layers of a single or multiple types would have the same property of noise filtration off an input sequence. Moreover it is possible to suggest that any neural network of several layers would share this behavior if it has RNN next to a last (linear) layer generating the network output.

The approximate predictive algorithm is governed by a multidimensional discrete map with the parameters determined by the weights and biases of the trained RNN only and does not require the input sequence. In all our numerical experiments we observe that the parameters of the trained network always lead to smooth dynamics generated by this reduced map. The same time setting these parameters to random real values sometimes produces nonsmooth and quite nontrivial dynamics including complex periodic trajectories. We do not observe chaotic dynamics but such possibility cannot be excluded. It is very important to understand what is special about the parameters of the trained network that they *always* produce smooth trajectory generated by both the original and approximate predictive schemes.

Another important aspect of RNN noise filtering is related to neuroscience. A noisy time series of three dimensional vectors is a good approximation of an object trajectory in space. The brain ability to predict a trajectory is one of the most important requirements for survival and this natural ability is highly developed. By default the brain should be able to predict trajectories based on incomplete or noisy data, and it has to do this with high reliability. Moreover, the predictions should be made for several objects simultaneously and it requires large resources. The trajectory prediction is usually considered as a two-stage process – first, the brain performs initial classification of the trajectory and then, in case when the organism should somehow react to this specific motion, a precise predictive mechanism is activated. If the available data is noisy both these stages would require more resources compared to processing of smooth trajectories. We hypothesize that there is an additional inexpensive (with small number of neurons) RNN that is activated first. It would effectively filter noise out and transfer a cleaned smooth trajectory segment to the classification and then to precise predictive networks. Note that in this case the latter networks resources can be greatly reduced.

Also we learned that the prediction process can be significantly accelerated by using the approximate algorithm proposed in the manuscript. It would be interesting to address a possibility of a physiological implementation of this scheme. If this algorithm does work in the brain then it is possible to hypothesize that the trajectory prediction of an object is done in two stages — first the existing trajectory segment is fed into the network and the first point is predicted. Then the input information can be forgotten and the brain predicts a few next points based on the approximate scheme. When a new input sequence is delivered by receptors a correction of predicted trajectory is performed. It saves resources and helps to resolve the

problem of prediction time minimization – there exists a range of lengths  $m$  of the input sequence for which the prediction quality is proportional to  $m$  thus the brain tends to increase the value of  $m$ . This increase requires a linearly proportional increase in prediction time when the standard algorithm is employed. A switch to the approximate algorithm allows significant reduction in the processing time without loss in the prediction quality.

In conclusion the predictive RNN can work as effective filter of the noisy time series. The essence of the effect is due to the fact that the predictive algorithm is a recursion of recursion which in majority of cases can be reduced to a simpler recursion.

## 9 Notation

Symbol and definition	Conditions	Meaning
$\mathcal{X} = \{\mathbf{x}_i\}$	$1 \leq i \leq N$	original time series with elements $\mathbf{x}_i$
$\mathbf{x}_i = \mathbf{g}(t_i)$		element $\mathbf{x}_i$ is a value of a function $\mathbf{g}$ at $t = t_i$
$d$	$d \geq 1$	dimension of $\mathbf{x}_i$
$\mathbf{g}(t) = \mathbf{g}_0(t) + a\boldsymbol{\xi}(t)$		$\mathbf{g}$ is a sum of a smooth function $\mathbf{g}_0$ and noise $\boldsymbol{\xi}$
$a$	$a \geq 0$	noise amplitude
$\mathbf{X}_{k,m} = \{\mathbf{x}_i\}$	$k+1 \leq i \leq k+m$	segment of $\mathcal{X}$ of the length $m$ starting with $\mathbf{x}_{k+1}$
$\bar{\mathbf{x}}_i$		$i$ -th element of $\mathcal{X}$ predicted by RNN
$\bar{\mathbf{X}}_{k+m,p} = \{\bar{\mathbf{x}}_i\}$	$k+m+1 \leq i \leq k+m+p$	sequence of $p$ predicted elements based on input $\mathbf{X}_k$
$\mathbf{X}^j$	$j > 0$	input to RNN at $j$ -th step of recursive prediction
$\mathbf{S}^j = \{\mathbf{s}_i^j\}$	$1 \leq i \leq m$	sequence of RNN states for input $\mathbf{X}^j$
$\mathbf{s}_i^j$		state vector at $j$ -th step of recursive prediction
$n$	$n \geq 1$	dimension of state vector $\mathbf{s}_i^r$
$\mathbf{W}_{ax}$	$a = i, m, f, o$	$n \times d$ matrix
$\mathbf{W}_{as}$	$a = i, m, f, o$	$n \times n$ matrix
$\mathbf{b}_a$	$a = i, m, f, o$	$n$ -dimensional vector
$\mathbf{W}$		$d \times n$ matrix
$\mathbf{b}$		$d$ -dimensional vector

Table 1: Symbols and corresponding definitions used in the manuscript.

## Acknowledgements

The author wishes to thank Vladimir Zverev for fruitful discussions.

## References

- [1] H. Georgiou, S. Karagiorgou et al, Moving object analytics: survey on future location & trajectory prediction methods, Technical report, 2018, [arXiv:1807.04639](#) [cs.LG].
- [2] P.R. Vlachas, W. Byeon et al, Data-driven forecasting of high-dimensional chaotic systems with long short-term memory networks, *Proc. R. Soc. A* 2017, **474**, 20170844.
- [3] Q. Li, R.-C. Lin, A new approach for chaotic time series prediction using recurrent neural networks, *Mathematical Problems in Engineering*, 2016, **2016**, ID 3542898.
- [4] R. Yu, S. Zheng, Y. Liu, Learning chaotic dynamics using tensor recurrent neural networks, *Proceedings of the ICML 17 Workshop on Deep Structured Prediction*, Sydney, Australia, PMLR 70, 2017.
- [5] S. Haykin (Ed.), *Kalman filtering and neural networks*, John Wiley, 2001.

- [6] K. Yeo, Short note on the behavior of recurrent neural network for noisy dynamical system, 2019, [arXiv:1904.05158](#) [cs.NE].
- [7] S. Hochreiter, J. Schmidhuber, Long-shotr term memory, Neural. Comput., 1997, **9**, 1735-1780.